GLOBAL BIOGEOCHEMICAL CYCLES, VOL. 14, NO. 2, PAGES 655-667, JUNE 2000

Equatorial nutrient trapping in biogeochemical ocean models: The role of advection numerics

Andreas Oschlies

Institut für Meereskunde an der Universität Kiel, Kiel, Germany

Abstract. The unrealistic accumulation of nutrients below the equatorial upwelling regions, termed "nutrient trapping" by *Najjar et al.* [1992], has been a major problem of first-generation oceanic carbon cycle models. Suggestions to eliminate this modeling problem include the consideration of dissolved organic nutrients and improvements to the underlying circulation field. This study shows that neither of these suggestions can be complete without a careful investigation of advection numerics. Using a high-resolution coupled biological-physical model of the North and equatorial Atlantic, it is demonstrated for standard central-difference advection (if a too coarse vertical resolution is used) as well as for upstream advection that numerical artifacts alone can lead to a systematic overestimation (by as much as 50%) of simulated subsurface nutrient concentrations in the equatorial upwelling region. A corollary of these results is that without a critical examination of the underlying advection numerics, nutrient trapping alone can no longer present an unchallenged justification for including dissolved organic matter in biogeochemical ocean models.

1. Introduction

First-generation models of oceanic biogeochemical cycles [*Toggweiler,* 1989; *Bacastow and Maier-Reimer,* 1991; *Najjar et al.*, 1992] failed to reproduce observed nutrient concentrations in the equatorial regions when run in particle-only mode. Simulated subsurface nutrient concentrations were as much as 50% higher than observed, a phenomenon most pronounced in the Pacific, but present also in the Atlantic Ocean. *Najjar et al.* [1992] showed that this model deficiency, which they called "nutrient trapping," could result from an interaction between upwelling of nutrient-rich waters that fuels intense primary production at the surface and shallow remineralization of organic matter within the equatorial upwelling region. In the concept of *Najjar et al.* [1992], nutrient trapping refers only to the zone from which water upwells. It does not necessarily imply an increase in the vertically integrated nutrient load of the equatorial waters.

So far, most attempts to resolve this model problem concentrated on apparent errors or oversimplifications in the ecological models used. It may have been an unfortunate coincidence that *Suzuki et al.* [1985] and *Sugimura and Suzuki* [1988], only a few years before the first incidence of nutrient trapping in biogeochemical ocean models, had reported measurements of unexpectedly high concentrations of dissolved organic carbon (DOC) and nitrogen (DON). When Redfield ratios were assumed to hold for dissolved organic matter (DOM) (as *Sugimura and Suzuki* [1988] had reported for C:N) and a corresponding similarly large pool of dissolved organic phosphate (DOP) was included in the models, both *Bacastow and Maier-Reimer* [1991] and *Najjar et al.* [1992] were able to reduce their high equatorial nutrient concentrations to approximately realistic levels. These studies assumed that a large fraction of new production went into the DOM pool (70% in the work by *Bacastow and Maier-Reimer* [1991], 80% in that of *Najjar et al.* [1992]) and that DOM lifetimes were of the order of 100 years. Given these assumptions, i.e., a large fraction of new production going into long-lived DOM following Redfield stochiometry, horizontal divergence of equatorial surface waters could carry phosphorus away from the strong upwelling region and thereby avoid nutrient trapping.

Although *Najjar et al.* [1992] already stated that the physical part of the coupled model had certain flaws, in particular, a too diffusive and too warm thermocline, they concluded that improving this apparent model deficiency was likely to make the problem of nutrient trapping even more severe, and they did not pursue this route any further. After the measurements of high DOC and DON concentrations had been withdrawn [*Suzuki,* 1993], *Anderson and Sarmiento* [1995] reexamined the

Paper number 1999GB001217.
0886-6236/00/1999GB001217$12.00

results of *Najjar et al.* [1992]. For the same circulation model and current fields they found that the nutrient problem could be circumvented using much smaller average DOP concentrations than those of *Najjar et al.* [1992]. While the portion of new production that went into DOP was changed only slightly from 80% to 50%, the assumed lifetime of DOP was reduced to $\sim$ 1 year at the ocean surface (increasing to a few thousand years at depth). The results showed still considerable misfits between the simulated and observed phosphate distribution that the authors concluded [*Anderson and Sarmiento*, 1995, p. 632] to be "primarily due to shortcomings in the physical model, rather than the biological model."

Bacastow and Maier-Reimer [1991] had already stated that without the high concentrations of DOC reported by *Sugimura and Suzuki* [1988], their first thought to explain the overestimated equatorial nutrient concentrations would have been that there was a problem with the physical model. After the withdrawal of the high DOC measurements, *Maier-Reimer* [1993] presented a new version of his biogeochemical model which did not include DOM, but which had an improved physical circulation. In this model the problem of nutrient trapping was, however, not much reduced with respect to the particle-only simulation of *Bacastow and Maier-Reimer* [1991]. In a subsequent study, *Six and Maier-Reimer* [1996] reintroduced DOC (and, via a C:P ratio of 122:1, also DOP) into the model, concentrating on the semilabile fraction with decay timescales $<$ 1 year. Together with the explicitly simulated evolution and advection of phytoplankton and zooplankton biomass, the DOC (and DOP) pool could reduce the equatorial nutrient trapping by a factor of ~ 2.

An inverse modeling study by *Matear and Holloway* [1995], on the other hand, suggested that with relatively small changes to the tropical advection velocities the model of *Bacastow and Maier-Reimer* [1991] was able to reach realistic nutrient concentrations in the North and equatorial Pacific without the need to introduce a speculative DOP compartment. In a recent paper, *Aumont et al.* [1999] demonstrated that nutrient trapping in the particle-only model of *Maier-Reimer* [1993] could be much reduced when the circulation field was taken from a higher-resolution primitive-equation model. They attributed the more realistic simulation of the nutrient fields to two improvements of the physical model: first, the horizontal grid resolution was increased from $\sim 4°$ of the first-generation models [*Bacastow and Maier-Reimer*, 1991; *Najjar et al.*, 1992] to 0.5° near the equator; second, their model included a turbulence closure scheme [*Gaspar et al.*, 1990]. They did, however, not discuss a third modification: the numerical treatment of advection. While *Bacastow and Maier-Reimer* [1991] and *Maier-Reimer* [1993] used upstream advection, *Aumont et al.* [1999] employed the less diffusive higher-order multidimensional positive definite advection transport algorithm (MPDATA) of *Smolarkiewicz* [1982, 1983] and *Smolarkiewicz and Clark* [1986]. Another scheme was used by *Najjar et al.* [1992] (and also by *Anderson and Sarmiento* [1995]), who applied the standard central-difference advection numerics to the biogeochemical tracers.

While previous attempts to reduce the overestimated equatorial nutrient concentrations in biogeochemical models had concentrated first on apparent errors in the simulated biology and partly also on possible deficiencies of the underlying circulation field, a numerical origin of the nutrient-trapping problem had first been suspected by *Oschlies and Garçon* [1999], (hereinafter referred to as OG99) for the case of upstream numerics. Because of artificial upwelling of nutrient-rich water at the closed southern wall of their model at 15°S, OG99 could, however, not rule out adverse effects of the boundary condition on equatorial nutrient fields. The present study uses a more appropriate southern boundary condition by restoring nitrate concentrations to the *Conkright et al.* [1994] climatology close to the artificial wall. Moreover, the analysis is extended to the central-differences advection scheme that has also been applied in first-generation biogeochemical models. The results presented in this study demonstrate that for a given circulation field the choice of the numerical advection scheme for biological tracers greatly influences the simulated equatorial nutrient fields. Differences obtained for different numerical discretizations but identical advection fields and identical ecosystem dynamics are of the same order of magnitude as those reported in earlier studies to be resulting from the consideration of DOM [*Six and Maier-Reimer*, 1996] or from improvements in the model physics [*Aumont et al.*, 1999]. Moreover, the sign of the differences is such that the numerical schemes and vertical grids used to represent tracer advection in earlier biogeochemical models may have enhanced (if not generated) nutrient trapping. It is suggested here that nutrient trapping may have had a primarily numerical origin and therefore cannot present a sound justification for including DOP (or DON) in biogeochemical models.

The paper is organized as follows: Section 2 will briefly present the model configuration used in this study. In section 3 it will be shown that the central-difference advection used by *Najjar et al.* [1992] as well as the upstream differencing of *Bacastow and Maier-Reimer* [1991] can both produce nutrient trapping which, for the same circulation field and the same ecosystem model, is much reduced when an (approximately) second-order advection scheme together with an appro-

priate vertical resolution are used. Implications for the role of DOM in biogeochemical modeling are discussed in the conclusion.

2. Model Description

The physical component of the coupled ecosystem-circulation model is based on the Geophysical Fluid Dynamics Laboratory's (GFDL) Modular Ocean Model (MOM) [*Pacanowski et al.*, 1991]. The present configuration is derived from the Community Modeling Effort (CME) model [*Bryan and Holland*, 1989] and covers the Atlantic Ocean between 15°S and 65°N with a grid spacing of 1/3° in meridional and 2/5° in zonal directions. While the original CME model had 30 levels in the vertical, a finer 37-level vertical grid is used for coupling with a simple nitrate, phytoplankton, zooplankton, detritus (NPZD) nitrogen-based pelagic ecosystem model (OG99). Turbulent vertical mixing in and below the surface mixed layer is modeled using the turbulent kinetic energy (TKE) closure of *Gaspar et al.* [1990] in the three-dimensional implementation proposed by *Blanke and Delecluse* [1993] and also employed by *Aumont et al.* [1999]. Different numerical advection schemes are available, presented in the respective sections herein.

The model is forced by monthly mean wind stress and heat flux data derived from the reanalysis project [*Gibson et al.*, 1997] carried out at the European Centre for Medium-Range Weather Forecasts (ECMWF). ECMWF data for the years 1989 to 1993 were used to construct the climatological mean seasonal forcing. The physical model was initialized with winter temperatures and salinities taken from the *Levitus* [1982] climatology and then integrated for 25 years before the ecosystem was coupled in. In contrast to the model of OG99, nitrate concentrations are restored to the *Conkright et al.* [1994] climatology at the southernmost (and northernmost) five grid points. The restoring timescale for nitrate is the same as that for temperature and salinity and decreases from 25 days at the innermost grid point to 5 days at the wall. No restoring is applied to phytoplankton and zooplankton or detritus.

The simple NPZD ecosystem model is a particle-only model that does not explicitly include DOM. Detritus sinks with a constant sinking speed ($5\,\mathrm{m\,d^{-1}}$) through the water column. With a detritus remineralization rate of $0.05\,\mathrm{d^{-1}}$ this corresponds to a particle remineralization depth scale of 100 m. Originally, this depth scale was chosen for the basin-scale model to closely resemble the vertical gradient in the Bermuda Atlantic Time series Study (BATS) sediment trap data [*Lohrenz et al.*, 1992]. Clearly, this simple description of particle export is not adequate for the deep ocean, and experiments with an improved parametrization of aggregation and sinking [*Kriest and Evans*, 1999] are now underway. According to the analysis presented by *Najjar et al.* [1992], nutrient trapping will increase with decreasing particle remineralization depth. In this respect the ecosystem model used here should be a perfect candidate to exhibit strong nutrient trapping. Note, however, that detritus not only sinks, but is additionally advected by the circulation field. An infinitely slowly sinking detritus compartment will in this context become indistinguishable from DOM.

3. Results

3.1. Nutrient Trapping Generated by CTCS Advection

In many ocean circulation models such as the GFDL MOM, the advection of temperature, salinity, and momentum is modeled using central differences both in space and in time (central in time, central in space (CTCS)). Among the main reasons for using the CTCS advection scheme are conceptual simplicity, little implicit diffusion, and $O(\Delta x^2)$ accuracy. A major drawback of central-difference advection is, however, the possible generation of undershoots and overshoots when sharp tracer gradients are advected. An instructive description of the CTCS scheme's inherent property to be dispersive, i.e., to generate overshoots and undershoots is given, for example, by *Webb et al.* [1998]. Adverse effects of such numerical noise are well known in physical models and have been investigated for some time [e.g., *Leonard*, 1979; *Weaver and Sarachik*, 1990; *Gerdes et al.*, 1991; *Hecht et al.*, 1998]. For biogeochemical models, CTCS advection is usually not applicable, because undershoots can generate negative tracer concentrations, which may in turn violate assumptions underlying the ecosystem equations (e.g., Michaelis-Menten kinetics). Among the biogeochemical models mentioned in the introduction, only the model of *Najjar et al.* [1992] (used again by *Anderson and Sarmiento* [1995]) employed CTCS advection. These models did not explicitly resolve ecological variables other than phosphate, and new production was simply modeled by restoring to observed surface phosphate concentrations. Hence negative tracer concentrations did not present a fundamental problem in the governing equations.

The negative phosphate concentrations that emerged in such models were discussed by *Najjar et al.* [1992] in terms of numerical dispersion caused by horizontal CTCS advection. A sufficient criterion for the absence of overshoots and undershoots is that the grid Péclet number, $Pe = |w|\Delta z/K_\rho$, for a velocity w, a grid spacing Δz, and a diffusivity K_ρ, is smaller than 2 (e.g., *Bryan et al.* [1975], who additionally discuss other sta-

bility criteria whose application in ocean circulation models is standard, but which must also be considered when running off-line biogeochemical models). While *Najjar et al.* [1992] pointed out that the criterion $Pe < 2$ was violated in many locations for the horizontal flow, they did not consider problems originating from vertical advection. *Weaver and Sarachik* [1990] had already demonstrated that a coarse vertical resolution as used by *Najjar et al.* [1992] (12 vertical levels) is not sufficient to suppress numerical overshoots and undershoots in the vertical if the standard central-differences advection scheme is used and realistic vertical diffusivities [$O(0.1\,\mathrm{cm^2\,s^{-1}})$] are applied. Even for models with a much higher vertical resolution, grid Péclet numbers for the vertical direction are generally still much larger than 2 and often exceed the grid Péclet numbers for the horizontal flow field [*Oschlies,* 1999].

A simple demonstration of the effect of CTCS advection to the ecosystem model of OG99 is not possible, because the ecological equations are ill-behaved for negative concentrations. As a substitute, a simple dye tracer is used. The tracer's initial concentration is set to 1 everywhere. Only in the surface layer of the model is the tracer subsequently set to 0 at every time step of ~ 30 min, to mimic rapid biogenic removal of nutrients in the light-lit upper ocean. The constellation is set to dilute the initial dye field, as there is no equivalent of remineralization of dye "consumed" at the surface. Two model experiments were run, differing only in vertical resolution: the first experiment uses the configuration of OG99 with 37 depth levels, the second one uses a reduced vertical resolution of 30 levels (i.e., the original CME model grid). These experiments are named C37 and C30, respectively. Reducing the vertical resolution further to the 12 levels of *Najjar et al.* [1992] has not been attempted here, because this would require con-

Table 1. Vertical Levels Used in Experiment C30

Model Level	Depth of Grid Point	Depth of Grid Box Bottom	Thickness of Grid Box
1	17.50	35.00	35.00
2	53.43	71.85	36.85
3	91.64	111.43	39.58
4	133.19	154.95	43.52
5	179.52	204.09	49.14
6	232.60	261.10	57.01
7	295.03	328.95	67.85
8	370.21	411.47	82.52
9	462.51	513.54	102.07
10	577.37	641.19	127.65
11	721.47	801.74	160.55
12	900.89	1000.04	198.30
13	1125.04	1250.04	250.00
14	1375.04	1500.04	250.00
15	1625.04	1750.04	250.00
16	1875.04	2000.04	250.00
17	2125.04	2250.04	250.00
18	2375.04	2500.04	250.00
19	2625.04	2750.04	250.00
20	2875.04	3000.04	250.00
21	3125.04	3250.04	250.00
22	3375.04	3500.04	250.00
23	3625.04	3750.04	250.00
24	3875.04	4000.04	250.00
25	4125.04	4250.04	250.00
26	4375.04	4500.04	250.00
27	4625.04	4750.04	250.00
28	4875.04	5000.04	250.00
29	5125.04	5250.04	250.00
30	5375.04	5500.04	250.00

Units are meters.

Table 2. Vertical Levels Used in Experiment C37

Model Level	Depth of Grid Point	Depth of Grid Box Bottom	Thickness of Grid Box
1	5.50	11.00	11.00
2	17.00	23.00	12.00
3	29.00	35.00	12.00
4	41.00	47.00	12.00
5	53.00	59.00	12.00
6	65.50	72.00	13.00
7	78.50	85.00	13.00
8	91.50	98.00	13.00
9	104.50	111.00	13.00
10	118.50	126.00	15.00
11	140.50	155.00	29.00
12	179.55	204.09	49.09
13	232.60	261.10	57.01
14	295.03	328.95	67.85
15	370.21	411.47	82.52
16	462.51	513.54	102.07
17	577.37	641.19	127.65
18	721.47	801.74	160.55
19	900.89	1000.04	198.30
20	1125.04	1250.04	250.00
21	1375.04	1500.04	250.00
22	1625.04	1750.04	250.00
23	1875.04	2000.04	250.00
24	2125.04	2250.04	250.00
25	2375.04	2500.04	250.00
26	2625.04	2750.04	250.00
27	2875.04	3000.04	250.00
28	3125.04	3250.04	250.00
29	3375.04	3500.04	250.00
30	3625.04	3750.04	250.00
31	3875.04	4000.04	250.00
32	4125.04	4250.04	250.00
33	4375.04	4500.04	250.00
34	4625.04	4750.04	250.00
35	4875.04	5000.04	250.00
36	5125.04	5250.04	250.00
37	5375.04	5500.04	250.00

Units are meters.

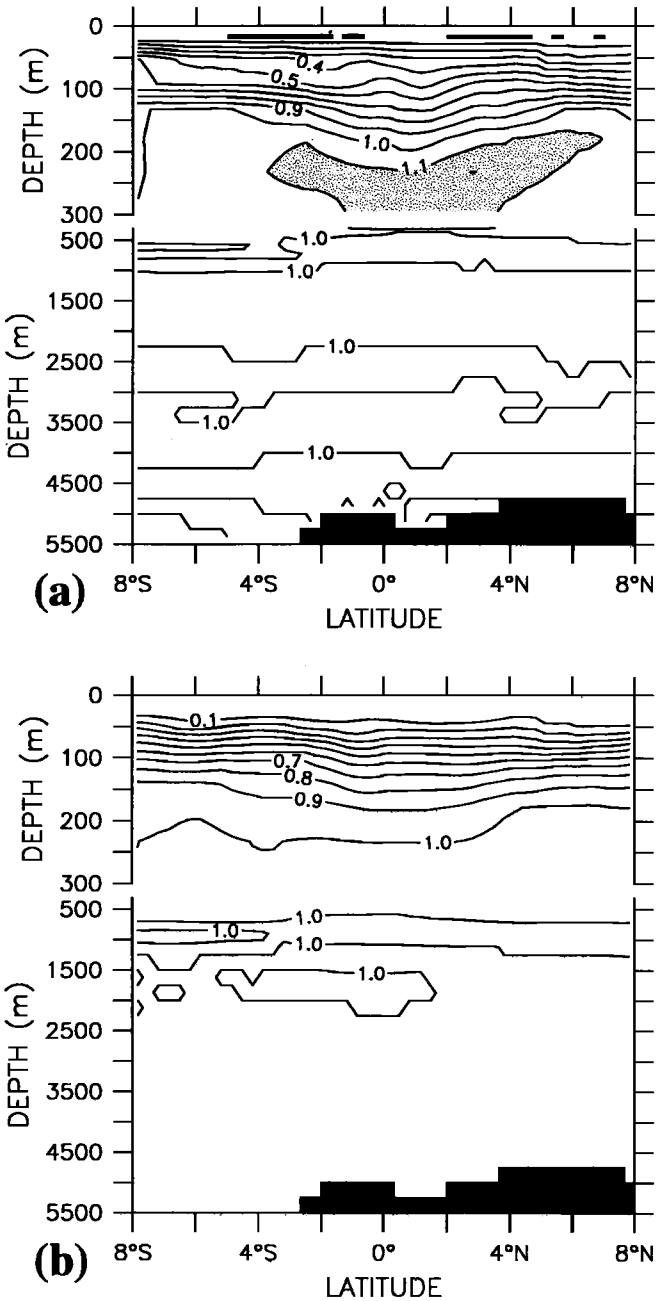

Figure 1. Zonally averaged annual mean dye concentration for the fifth year of the simulation. (a) Experiment C30 with a vertical resolution of 30 levels. (b) Experiment C37 with 37 levels in the vertical. Regions in which dye concentrations reach more than 110% of the initial value are shaded. The thick solid line close to the surface in Figure 1a is the zero contour. Note the change in vertical scale at a depth of $z = 300\,\mathrm{m}$.

siderable changes to the model topography. The two experiments C30 and C37 use exactly the same bottom topography, and their vertical grids differ only in the upper 150 m, where 4 levels are situated in experiment C30 (Table 1) in contrast to 11 levels in run C37 (Table 2). Note that the thickness of the surface layer in which the dye is set to 0 differs among the two models. The very rapid dye "uptake" nevertheless ensures that in both model experiments the entire surface mixed layer is essentially dye depleted. No restoring is applied to the dye tracer at the closed northern and southern walls of the model.

Both models are integrated for 5 years, using CTCS advection for the dye tracer. Figure 1 displays zonally averaged meridional sections of the passive dye tracer field. Although there is no explicit formulation to increase dye concentrations to values larger than 1, considerably larger tracer concentrations accumulate below the equatorial upwelling region in experiment C30. A zonal section along the equator shows (Figure 2) that maximum overshoots develop in the eastern basin where dye concentrations exceed the initial values by more than half. This pattern is similar to the enhanced phosphate concentrations described by *Najjar et al.* [1992] in a 12-level model, although the depth range at which the anomaly develops is shallower in the C30 experiment, which has more than twice the vertical resolution. Refining the vertical resolution further as in experiment C37, dye overshoots are reduced to less than a tenth of the initial concentration everywhere. A similar reduction of numerical overshoots produced by the CTCS algorithm on switching from the vertical grid of experiment C30 to that of experiment C37 was reported for the equatorial salinity field [*Oschlies,* 1999]. That study concluded that the most realistic distributions of physical tracers were reached when high vertical resolution was combined with an upstream-weighted advection scheme. However, general consensus about an optimal distribution of computer resources among grid resolution and advection numerics has not yet emerged.

The above simulation shows that a tracer anomaly similar to that associated with nutrient trapping can develop solely because of numerical dispersion. While setting the surface concentrations to 0 may be viewed as biological consumption of the dye, there is no analogue for particle export and remineralization at depth included in this model. All dye removed is simply taken out of the model. Although 0% of such "new production" is put into export, the model produces equatorial "dye trapping" with overestimated tracer concentrations by as much as 50% in experiment C30.

3.2. Nutrient Trapping Generated by Upstream Advection

Among the advection schemes presently available (see *Hecht et al.* [1998] for a recent discussion), upstream differencing is computationally cheapest, and because it is also strictly monotonic and therefore conserves positive tracer concentrations, it has been widely used in three-dimensional pelagic ecosystem models [e.g., *Ba-*

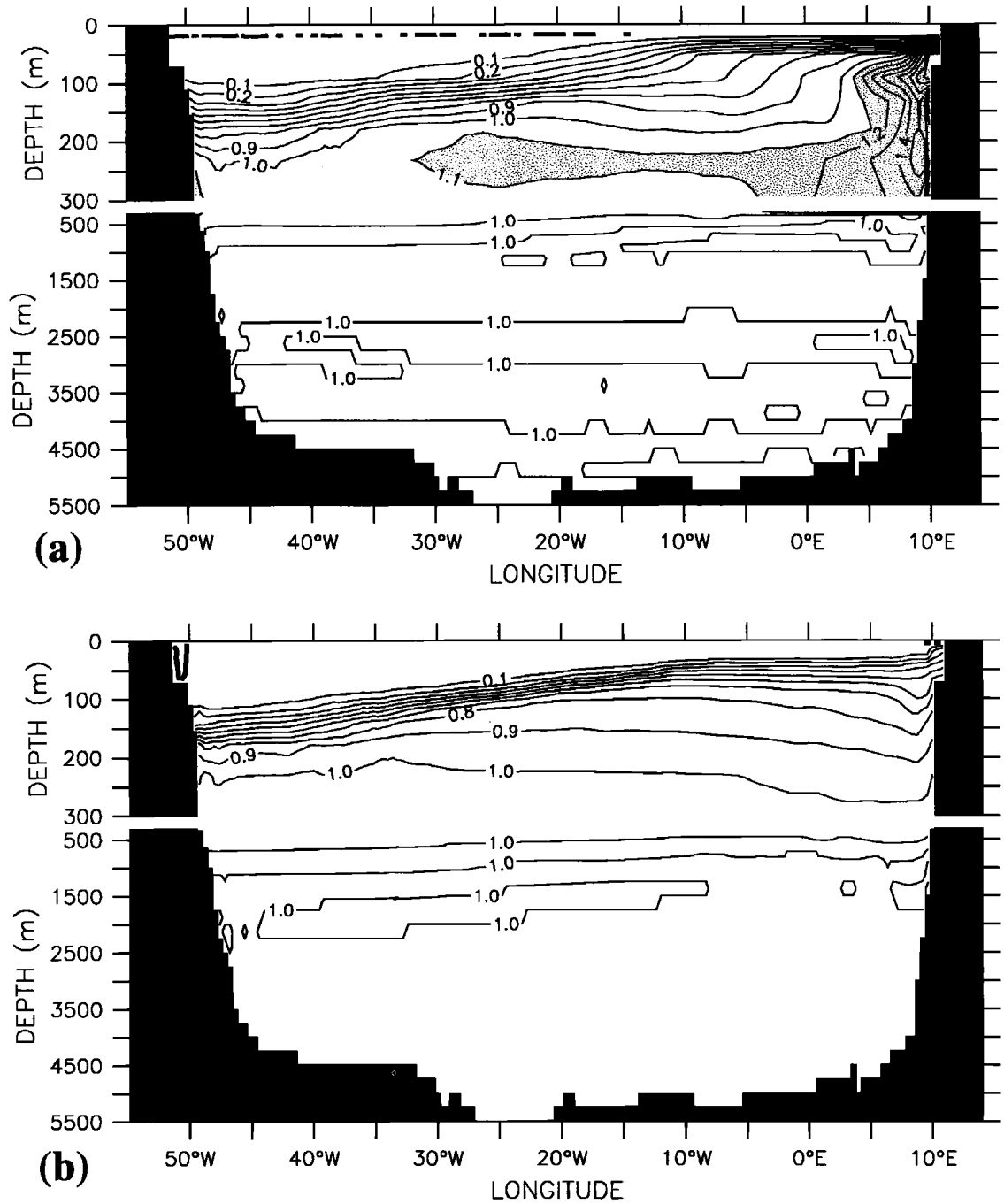

Figure 2. Zonal section of simulated dye concentrations along the equator, meridionally averaged from 4°S to 4°N, temporally averaged over the fifth year of the respective model run. (a) Experiment C30 with a vertical resolution of 30 levels. (b) Experiment C37 with 37 levels in the vertical. Regions in which dye concentrations reach more than 110% of the initial value are shaded. The thick solid line close to the surface is the zero contour. Note the change in vertical scale at a depth of $z = 300\,\mathrm{m}$.

castow and Maier-Reimer, 1991; *Maier-Reimer*, 1993; *Sarmiento et al.*, 1993; *Six and Maier-Reimer*, 1996]. A major disadvantage of the upstream scheme, however, is its large implicit diffusion. OG99 compared upstream advection with the multidimensional positive-definite, central-differences (MPDCD) scheme of *Lafore et al.* [1998]. The MPDCD scheme is based on central differences (CTCS) but computes flux limiters, ensuring that tracer fluxes leaving a grid box cannot completely empty this box during one time step (see the appendix

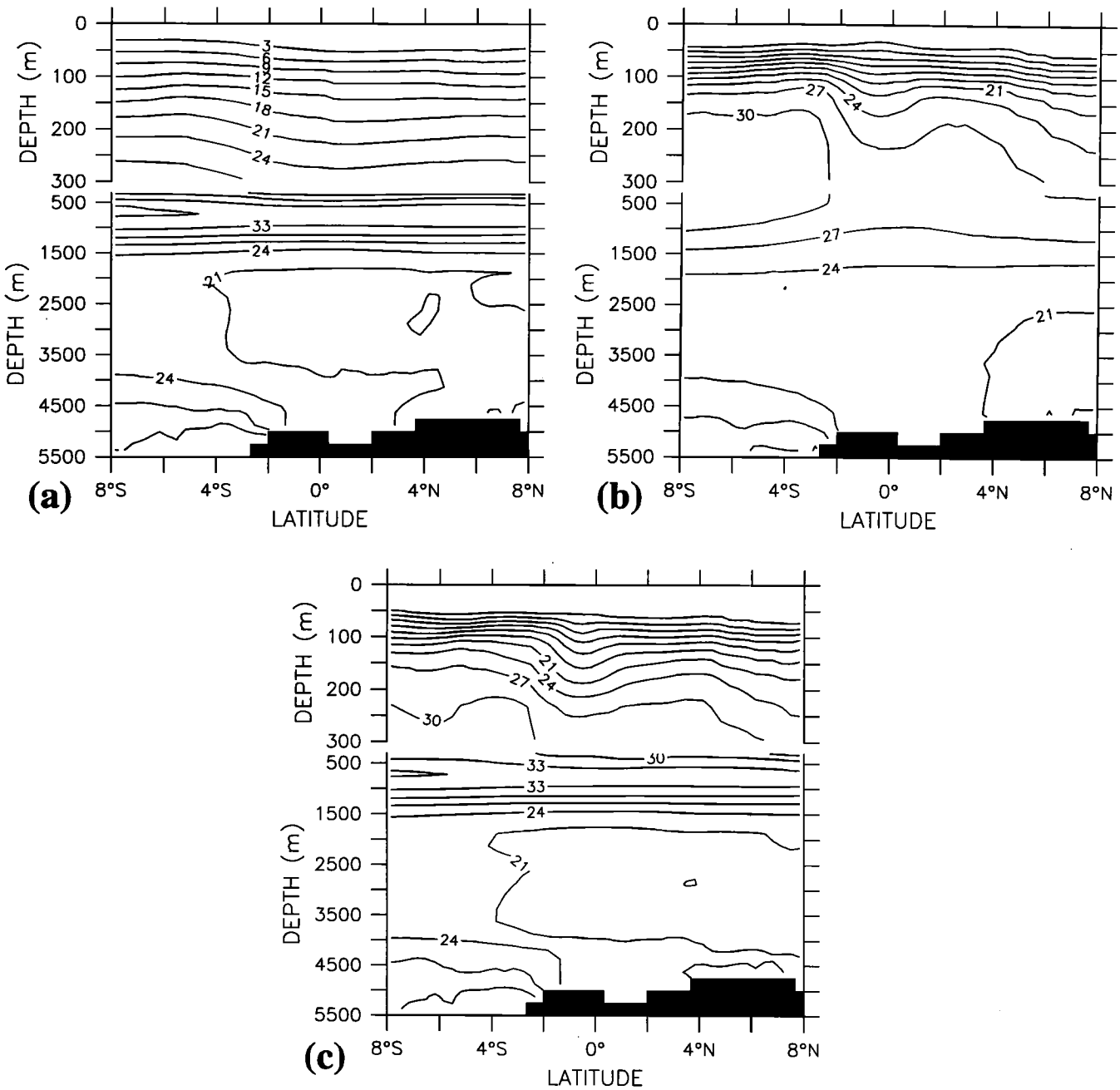

Figure 3. Zonally averaged annual mean nitrate concentration in the equatorial Atlantic. (a) Data of *Conkright et al.* [1994]. (b) Year 7 of experiment 1 with upstream advection. (c) Year 7 of experiment 2 with multidimensional positive-definite, central-differences (MPDCD) advection. Note the change in vertical scale at a depth of $z = 300\,\mathrm{m}$.

of OG99 for a more detailed description of the algorithm). Being derived from the CTCS scheme, MPDCD advection may nevertheless generate overshoots similar to those described in the previous section. Because the vertical grid employed by OG99 is that of experiment C37, nutrient trapping caused by numerical dispersion of the MPDCD scheme can be expected to be small (Figures 1b and 2b).

OG99 had already applied upstream and MPDCD advection to identical advecting flow fields and found a dramatic increase in the nutrient transport into the euphotic zone when switching from MPDCD to upstream advection. This increase was most pronounced in the equatorial upwelling region. It was caused by the large

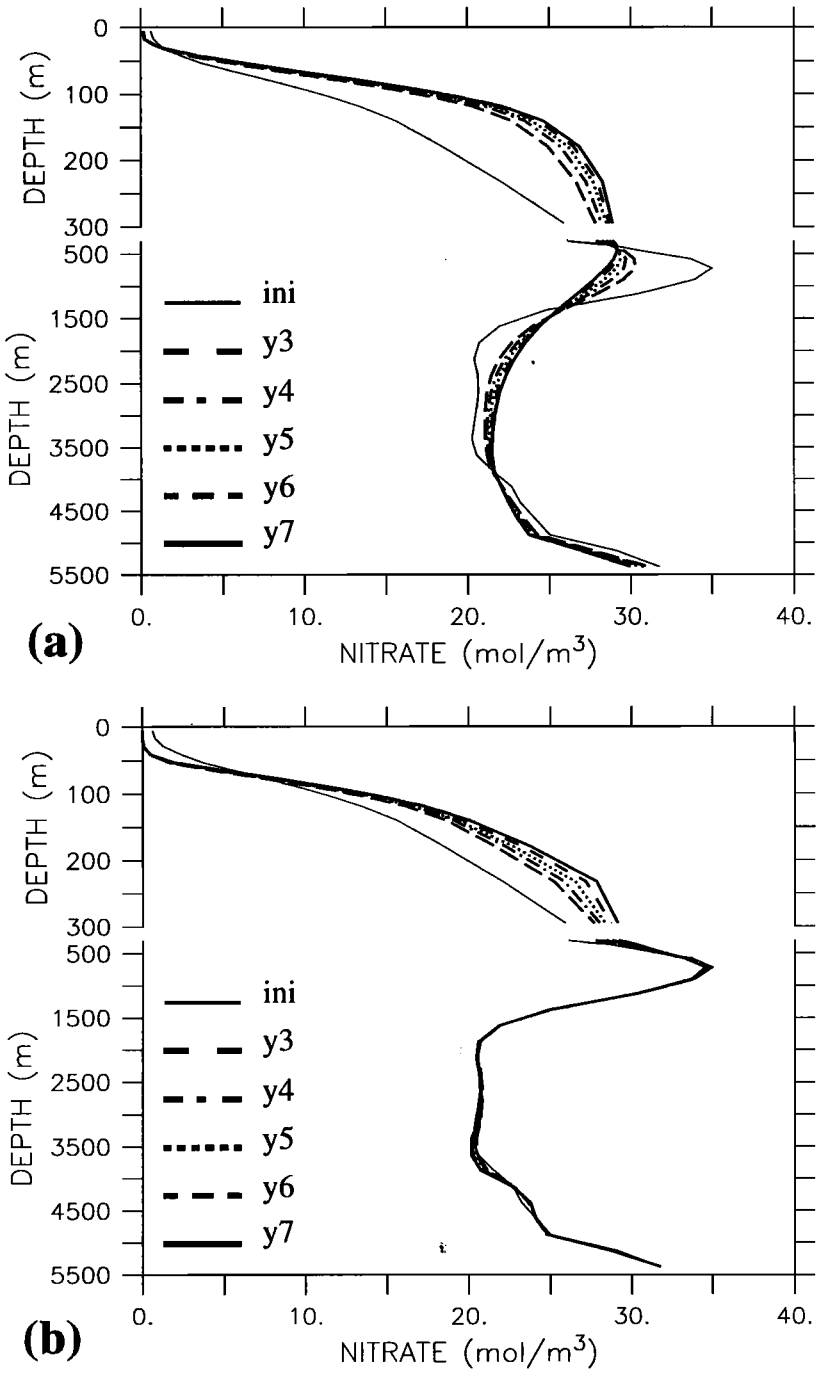

Figure 4. Annual mean nitrate profiles, averaged zonally from 80°W to 14°E and meridionally from 4°S to 4°N. Profiles are shown for the *Conkright et al.* [1994] nitrate field used to initialize the coupled biological-physical model, as well as for years 3 to 7 of the simulation. (a) Experiment 1 with upstream advection. (b) Experiment 2 with MPDCD advection. Note the change in vertical scale at a depth of $z = 300\,\mathrm{m}$.

implicit vertical diffusivities, which to leading order are given by $|w|\Delta z/2$ for a vertical velocity w and a vertical grid spacing Δz. OG99 showed that in their model configuration these implicit diffusivities were up to 1 to 2 orders of magnitude larger than explicit diffusivities computed by a turbulence closure scheme that had been tuned to comply with in situ measurements of diapycnal diffusion. Artificial upwelling of nitrate-rich water at the closed model boundary at 15°S detained OG99 from completely isolating the effect of the advection nu-

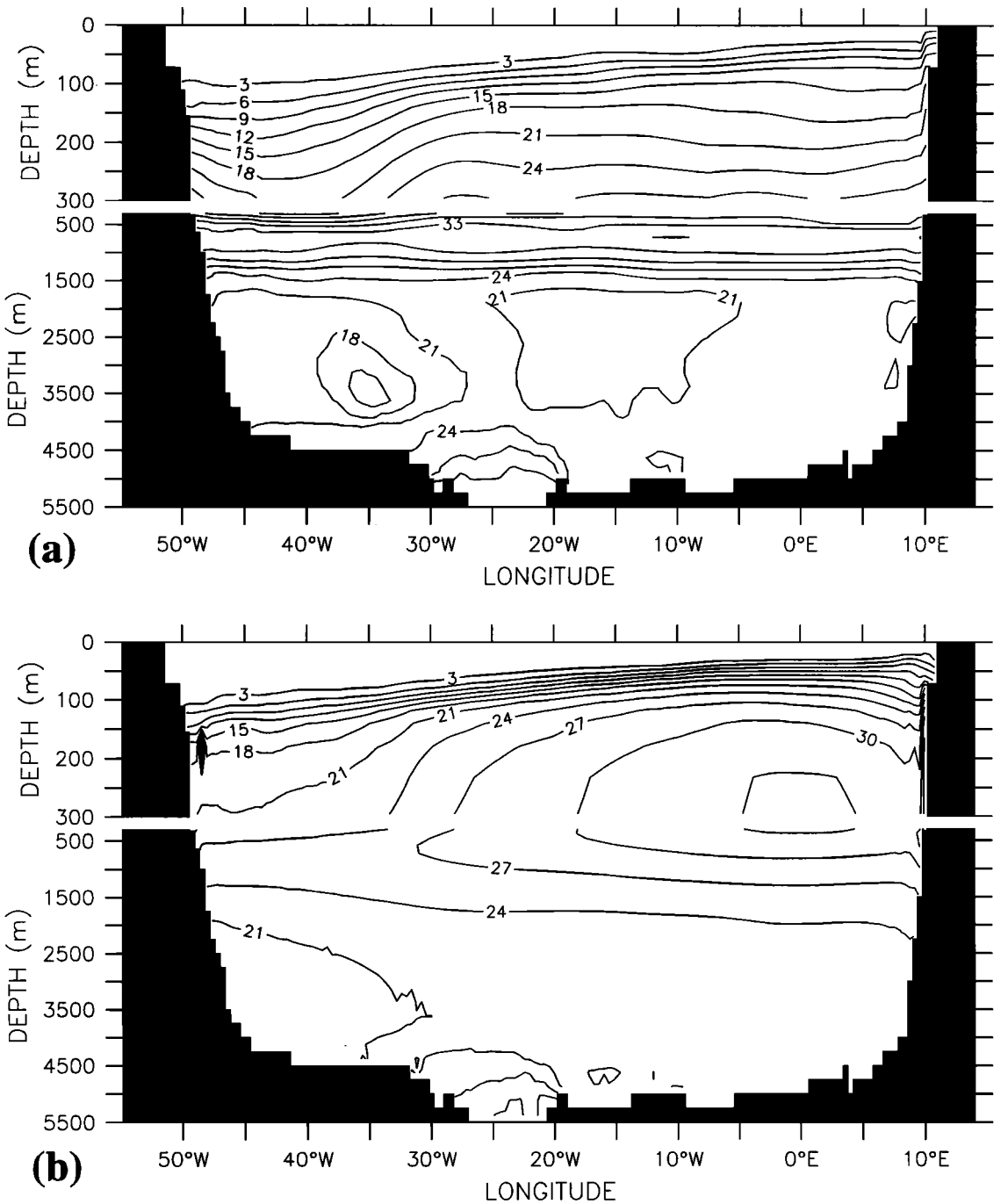

Figure 5. Zonal section of annual mean nitrate concentrations along the equator, meridionally averaged from 4°S to 4°N. (a) Data of *Conkright et al.* [1994]. (b) Year 7 of experiment 1 with upstream advection. (c) Year 7 of experiment 2 with MPDCD advection. Note the change in vertical scale at a depth of $z = 300\,\mathrm{m}$.

merics on the simulated tropical nitrate field. For this reason, nitrate concentrations in the upwelling region at the closed southern boundary are now restored to the *Conkright et al.* [1994] climatological data. In addition, the simulation period is extended from 3 years (OG99) to 7 years.

Results are shown for two experiments: the first uses upstream advection, the second employs the higher-order MPDCD advection scheme for biological tracers. Both experiments use CTCS advection for physical tracers, both are started from the same initial conditions, and both use the same atmospheric forcing.

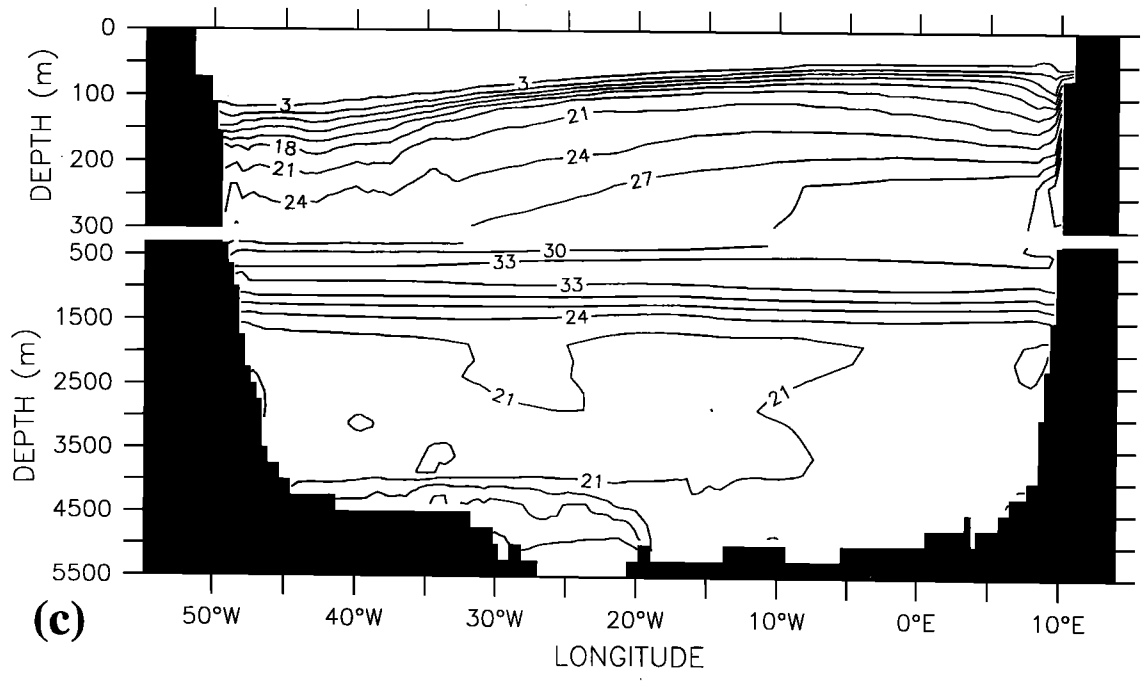

Figure 5. (continued)

Physical properties, in particular, the advecting velocity field, are thus identical in both experiments. As discussed by OG99, the strength of the equatorial upwelling as well as the simulated equatorial current system agree reasonably well with observational estimates.

Figure 3 shows a zonal average over the tropical Atlantic of the climatological nitrate field of *Conkright et al.* [1994], used to initialize the ecosystem model, together with the annual mean nitrate concentrations simulated by the two experiments. Obviously, the nitrate maximum associated with Antarctic Intermediate Water (AAIW) centered at a depth of $\sim$ 800 m is eroded by the action of the highly diffusive upstream scheme (Figure 3b), resulting in considerable upward displacements of nitrate-concentration isopleths above the core of the AAIW. Not all diffusive transport is directed toward the ocean surface, though. There is also a slight increase in nitrate concentrations in the deep ocean. Figure 3c shows the same section for the second experiment with upstream differencing being replaced by the MPDCD advection scheme. Here the nitrate maximum of the AAIW is much better conserved, and nitrate concentrations in and below the AAIW remain virtually unchanged with respect to the initalization field (Figure 3a). Only in the upper 300 m is there a sharpening of the nitracline and an associated increase of nitrate concentrations in the 100–300 m depth range. This difference with respect to the climatological nitrate field may not exclusively be caused by deficiencies of the numerical model, but may to some extent arise from the large smoothing applied to the atlas data. Individual station data also show nitrate concentrations lower than those in the model below $\sim$ 150 m, but the observed strength of the nutricline is very similar to that simulated by the model. Had we taken the nitrate concentrations from the third year of the respective simulation, Figure 3 would very closely resemble the earlier results reported by OG99. This suggests that the formulation of the southern boundary condition (no restoring of nitrate by OG99 versus restoring in the present study) is not overly critical for the simulated equatorial nitrate field. It must be noted, though, that even after 7 years of the coupled model integration, equatorial nitrate concentrations have not fully reached a climatologically steady state. This can be seen in the temporal evolution of the annual mean equatorial nitrate profiles for both upstream and MPDCD advection displayed in Figure 4. In the seventh year of the simulation, vertically integrated equatorial (60°-14°E, 4°S-4°N) nitrate stocks increase by 0.06% per year in the MPDCD run and by 0.14% per year in the upstream experiment. Absolute estimates of the magnitude of the simulated subsurface nitrate concentrations in the tropical Atlantic must therefore be viewed critically.

Zonal sections along the equator are shown in Figure 5. Both the climatological data and the two simulations display a eastward shallowing of the nitracline parallel to the sloping isopycnals and the path of the Equatorial Undercurrent. As a result, nitrate concentrations at any given depth level in the upper equatorial ocean tend to be highest in the east. Both *Bacastow and Maier-Reimer* [1991] and *Najjar et al.* [1992]

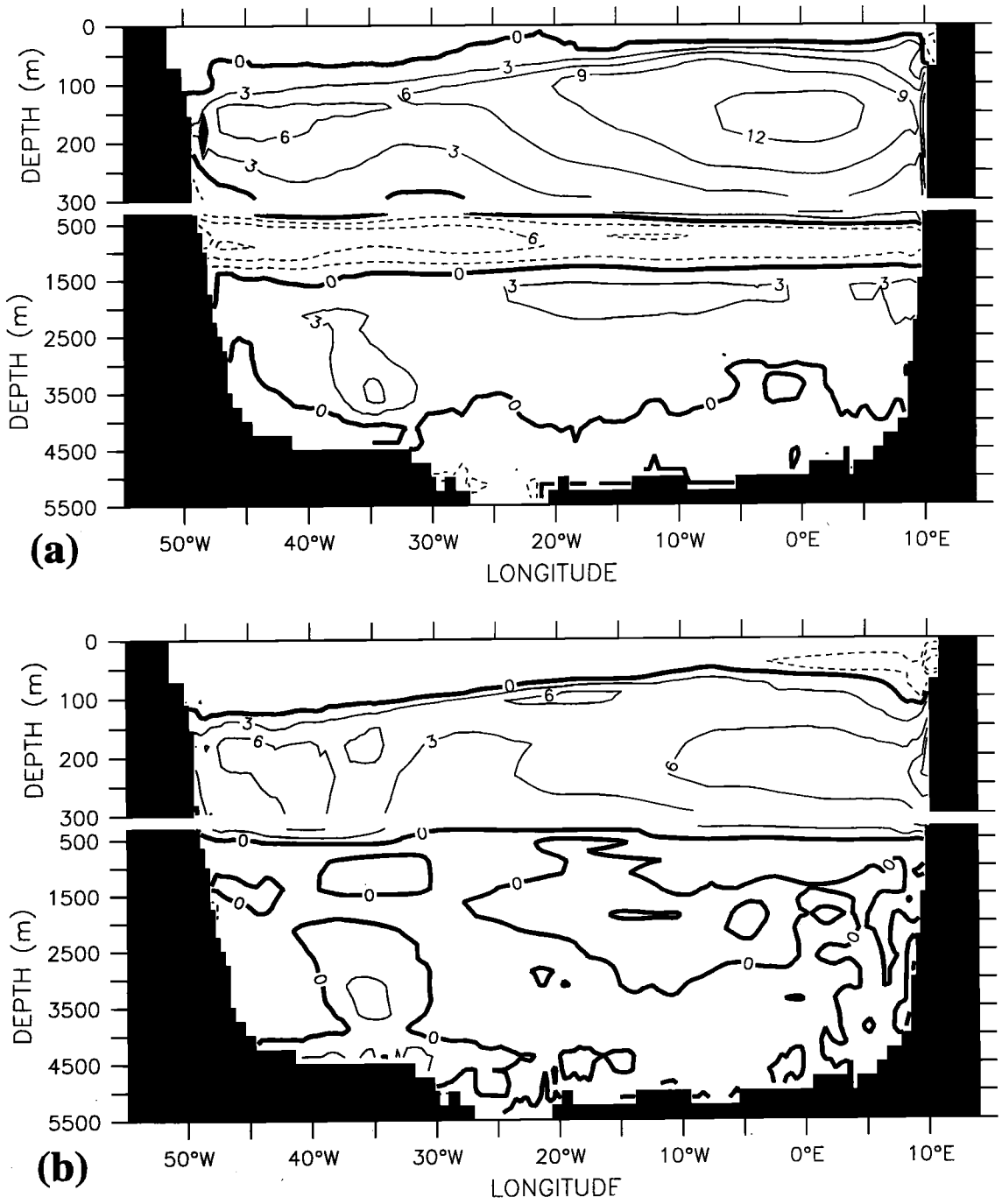

Figure 6. Zonal section of deviations in the simulated nitrate field from the data of *Conkright et al.* [1994]. (a) Year 7 of experiment 1 with upstream advection. (b) Year 7 of experiment 2 with MPDCD advection. All values represent meridional averages between 4°S and 4°N. Note the change in vertical scale at a depth of $z = 300\,\mathrm{m}$.

noted that nutrient trapping was largest in the eastern tropical oceans. A similar pattern is clearly visible in the upstream experiment (Figure 5b), but it is also present in a much reduced form in the MPDCD run (Figure 5c). To achieve a better quantification of the impact of the different advection numerics, Figure 6 shows the deviations of the respective simulated nitrate fields from the *Conkright et al.* [1994] climatology. While upstream advection leads to an overestimation by more than $12\,\mathrm{mmol\,NO_3\,m^{-3}}$ (or 50%, which is

about the size of nutrient trapping in the earlier model simulations of *Bacastow and Maier-Reimer* [1991] and *Najjar et al.* [1992]) in the eastern tropical Atlantic, the overstimation is only about half as large in the MPDCD run.

4. Discussion and Conclusions

The results presented herein demonstrate that the choice of advection numerics alone can substantially affect the magnitude of equatorial nutrient trapping in biogeochemical ocean models. Apart from the work of *Aumont et al.* [1999] almost all previous model studies used either upstream numerics or CTCS advection on a rather coarse vertical grid. Central differencing, unless applied on a fine enough vertical grid, as well as upstream advection both tend to overestimate subsurface nutrient concentrations in the equatorial upwelling region. Although the effect is similar in both cases, its cause is different for the two advection schemes: CTCS advection has no implicit diffusion, but its inherent numerical dispersion can generate considerable overshoots and undershoots. Upstream advection, on the other hand, is monotonic and hence does not generate overshoots or undershoots, but its high implicit diffusion can yield unrealistically large tracer fluxes. Both numerical problems are largest when the advective velocity is large with an orientation parallel to large tracer gradients. Such a condition is generally met in the equatorial upwelling.

For the high-resolution model used here, these numerical artifacts can lead to numerically generated nitrate maxima in the eastern equatorial Atlantic exceeding climatological values by $\sim 50\%$ unless a fine enough vertical grid and an appropriate advection scheme are used. This is similar to the magnitude of nutrient concentration overestimates in earlier studies [*Bacastow and Maier-Reimer,* 1991; *Najjar et al.,* 1992] and suggests that at least part of the then observed nutrient trapping was due to the chosen advection numerics and, in the case of CTCS numerics, the coarse vertical resolution. However, even in the MPDCD experiment of the high-(vertical)-resolution model and also in the model experiments reported by *Aumont et al.* [1999], who employed another higher-order advection scheme, nitrate concentrations are still too high (by up to 20%) in the tropical Atlantic. This is similar to the overestimate simulated by the particle-only model of the equatorial Pacific by *Chai et al.* [1996] who also used a relatively fine vertical resolution with 17 levels in the upper 300 m. The issue of nutrient trapping cannot therefore be considered completely resolved yet.

It remains a problem that thus far there is no particle-only ecosystem model that does not show signs of equatorial nutrient trapping. Multiple causes may explain this behavior; the neglect of DOM may be one of them. Overestimated nitrate concentrations in the tropical Atlantic may, for example, be related to the shallow remineralization depth scale (100 m) chosen. Other serious deficiencies of simple ecosystem model formulations cannot be ruled out either. The ecosystem model presented here has been tuned mainly against observations in midle and high latitudes, and substantial shortcomings have been identified, for example, in the subtropical gyre [*Oschlies et al.*, 2000]. In this respect the quantitative results of this study must still be viewed with some caution.

The relative differences in equatorial nutrient concentrations found between runs using different advection numerics are of the same order of magnitude as those reached in previous studies either by adding DOM [*Six and Maier-Reimer,* 1996] or by improving the oceanic circulation model [*Aumont et al.,* 1999]. It is suggested here that such numerical problems should be sorted out before attempting to correct for a mismatch between model results and observations by adjusting the ecosystem model formulation. For the time being, model-derived conclusions about the importance of DOM in the oceanic nutrient cycles must be considered as premature.

Acknowledgments. I thank Paul Kähler and Wolfgang Koeve for many clarifying discussions and critical reviews of an earlier version of the manuscript. Ray Najjar and two anonymous referees also provided very constructive comments that helped to improve the presentation. This study is a contribution to the German JGOFS program.

References

Anderson, L. A., and J. L. Sarmiento, Global ocean phosphate and oxygen simulations, *Global Biogeochem. Cycles, 9*, 621–636, 1995.

Aumont, O., J. C. Orr, P. Monfray, G. Madec, and E. Maier-Reimer, Nutrient trapping in the equatorial Pacific: The ocean circulation solution, *Global Biogeochem. Cycles, 13*, 351–370, 1999.

Bacastow, R., and E. Maier–Reimer, Dissolved organic carbon in modelling oceanic new production, *Global Biogeochem. Cycles, 5*, 71–85, 1991.

Blanke, B., and P. Delecluse, Variability of the tropical Atlantic Ocean simulated by a general circulation model with two different mixed–layer physics, *J. Phys. Oceanogr., 23*, 1363–1388, 1993.

Bryan, F. O., and W. R. Holland, A high resolution simulation of the wind– and thermohaline–driven circulation in the North Atlantic Ocean, in *Parameterization of Small–Scale Processes*, edited by P. Müller and D. Henderson, pp. 99–115, Hawaii Inst. of Geophys., Manoa, 1989.

Bryan, K., S. Manabe, and R. C. Pacanowski, A global ocean-atmosphere climate model, part II, the oceanic solution, *J. Phys. Oceanogr., 5*, 30–46, 1975.

Chai, F., R. T. Barber, and S. T. Lindley, Origin and maintenance of high nutrient condition in the equatorial Pacific, *Deep Sea Res., Part II, 43*, 1031–1064, 1996.

Conkright, M. E., S. Levitus, and T. P. Boyer, *World Ocean Atlas 1994*, vol. 1, *Nutrients*, Natl. Environ. Satell. Data

and Inf. Serv., Natl. Oceanic and Atmos. Admin., Silver Spring, Md., 1994.

Gaspar, P., Y. Gregoris, and J.-M. Lefevre, A simple eddy kinetic energy model for simulations of the oceanic vertical mixing: Tests at station Papa and Long–Term Upper Ocean Study site, *J. Geophys. Res.*, *95*, 16,179–16,193, 1990.

Gerdes, R., C. Köberle, and J. Willebrand, The influence of numerical advection schemes on the results of ocean general circulation models, *Clim. Dyn.*, *5*, 211–226, 1991.

Gibson, J. K., P. Kallberg, S. Uppala, A. Hernandez, A. Nomura, and E. Serrano, ERA description, Rep. Ser. 1, 72pp., ECMWF Re-Analysis Project, Eur. Cent. for Medium-Range Weather Forecasting, Reading, England, 1997.

Hecht, M. W., F. O. Bryan, and W. R. Holland, A consideration of tracer advection schemes in a primitive equation ocean model, *J. Geophys. Res.*, *103*, 3301–3321, 1998.

Kriest, I., and G. T. Evans, Respresenting phytoplankton aggregates in biogeochemical models, *Deep Sea Res., Part I*, *36*, 1841–1859, 1999.

Lafore, J.-P., et al., The Meso-NH atmospheric simulation system, I, Adiabatic formulation and control simulations, *Ann. Geophys.*, *16*, 90–109, 1998.

Leonard, B. P., 1979: A stable and accurate convective modelling procedure based on quadratic upstream interpolation, *Comput. Methods Appl. Mech. Eng.*, *19*, 59–98, 1979.

Levitus, S., Climatological atlas of the world ocean. *NOAA Prof. Pap. 13*, 173 pp, U.S. Gov. Print. Off., Washington, D.C., 1982.

Levitus, S., R. Burgett, and T. Boyer, *World Ocean Atlas 1994*, vol. 3, *Salinity*, *NOAA Atlas NESDIS 3*, 111 pp, Natl. Oceanic and Atmos. Admin., Silver Spring, Md., 1994.

Lohrenz, S. E., G. A. Knauer, V. L. Asper, M. Tuel, A. F. Michaels, and A. H. Knap, Seasonal variability in primary production and particle flux in the northwestern Sargasso Sea: US JGOFS Bermuda Atlantic Time-Series Study, *Deep Sea Res., Part A*, *39*, 1373–1391, 1992.

Maier–Reimer, E., Geochemical cycles in an ocean general circulation model: Preindustrial tracer distribution, *Global Biogeochem. Cycles*, *7*, 645–677, 1993.

Matear, R. J., and G. Holloway, Modeling the inorganic phosphorus cycle of the North Pacific using an adjoint data assimilation model to assess the role of dissolved organic phosphorus, *Global Biogeochem. Cycles*, *9*, 101–119, 1995.

Najjar, R. G., J. L. Sarmiento, and J. R. Toggweiler, Downward transport and fate of organic matter in the ocean: simulations with a general circulation model, *Global Biogeochem. Cycles*, *6*, 45–76, 1992.

Oschlies, A., An unrealistic high-salinity tongue simulated in the tropical Atlantic: Another example for the need of a more careful treatment of vertical discretizations in OGCMs, *Ocean Modell.*, *1*, 101–109, 1999.

Oschlies, A., and V. Garçon, An eddy-permitting coupled physical-biological model of the North Atlantic, 1, Sensitivity to physics and numerics, *Global Biogeochem. Cycles*, *13*, 135–160, 1999.

Oschlies, A., W. Koeve, and V. Garçon, An eddy-permitting coupled physical-biological model of the North Atlantic, 2, Ecosystem dynamics and comparison with satellite and JGOFS local studies data, *Global Biogeochem. Cycles*, in press, 2000.

Pacanowski, R., K. Dixon, and A. Rosati, The G.F.D.L Modular Ocean Model users guide version 1, *Tech. Rep. 2*, GFDL Ocean Group, Geophys. Fluid Dyn. Lab., Princeton, N. J., 1991.

Sarmiento, J. L., R. D. Slater, M. J. R. Fasham, H. W. Ducklow, J. R. Toggweiler, and G. T. Evans, A seasonal three–dimensional ecosystem model of nitrogen cycling in the North Atlantic euphotic zone, *Global Biogeochem. Cycles*, *7*, 417–450, 1993.

Six, K. D., and E. Maier-Reimer, Effects of plankton dynamics on seasonal carbon fluxes in an ocean general circulation model, *Global Biogeochem. Cycles*, *10*, 559–583, 1996.

Smolarkiewicz, K. P, The multidimensional Crowley advection scheme, *Mon. Weather Rev.*, *110*, 1968–1983, 1982.

Smolarkiewicz, K. P, A simple positive advection scheme with small implicit diffusion, *Mon. Weather Rev.*, *111*, 479–486, 1983.

Smolarkiewicz, K. P, and T. L. Clark, The multidimensional positive definite advection transport algorithm: Further development and applications, *J. Comput. Phys.*, *67*, 396–438, 1986.

Sugimura, Y., and Y. Suzuki, A high-temperature catalytic oxidation method for the determination of non-volatile dissolved organic carbon in seawater by direct injection of a liquid sample, *Mar. Chem.*, *24*, 105–131, 1988.

Suzuki, Y., On the measurement of DOC and DON in seawater, *Mar. Chem.*, *41*, 287–288, 1993.

Suzuki, Y., Y. Sugimura, and T. Itoh, A catalytic oxidation method for the determination of total nitrogen dissolved in seawater, *Mar. Chem.*, *16*, 83–97, 1985.

Toggweiler, J. R., New production: History, methods, problems, in *Productivity of the Ocean: Present and Past*, edited by W. H. Berger, V. S. Smetacek, and G. Wefer, pp85–97, John Wiley, New York, 1989.

Weaver, A. J., and E. S. Sarachik, On the importance of vertical resolution in certain ocean general circulation models, *J. Phys. Oceanogr.*, *20*, 600–609, 1990.

Webb, D. J., B. A. De Cuevas, and C. S. Richmond, Improved advection schemes for ocean models, *J. Atmos. Ocean. Techn.*, *15*, 1171–1187, 1998.

A. Oschlies, Institut für Meereskunde an der Universität Kiel, Düsternbrooker Weg 20, 24105 Kiel, Germany. (aoschlies@ifm.uni-kiel.de)

(Received August 24, 1999; revised December 28, 1999; accepted January 6, 2000.)